

14 Mar 1991, 10:30 am - 12:30 pm

## An Elastoplastic Model for Sand Liquefaction

Limin Zhang

*Chengdu University of Science and Technology, China*

Ting Hu

*Chengdu University of Science and Technology, China*

Follow this and additional works at: <https://scholarsmine.mst.edu/icrageesd>



Part of the [Geotechnical Engineering Commons](#)

### Recommended Citation

Zhang, Limin and Hu, Ting, "An Elastoplastic Model for Sand Liquefaction" (1991). *International Conferences on Recent Advances in Geotechnical Earthquake Engineering and Soil Dynamics*. 3. <https://scholarsmine.mst.edu/icrageesd/02icrageesd/session03/3>



This work is licensed under a [Creative Commons Attribution-Noncommercial-No Derivative Works 4.0 License](#).

This Article - Conference proceedings is brought to you for free and open access by Scholars' Mine. It has been accepted for inclusion in International Conferences on Recent Advances in Geotechnical Earthquake Engineering and Soil Dynamics by an authorized administrator of Scholars' Mine. This work is protected by U. S. Copyright Law. Unauthorized use including reproduction for redistribution requires the permission of the copyright holder. For more information, please contact [scholarsmine@mst.edu](mailto:scholarsmine@mst.edu).



# An Elastoplastic Model for Sand Liquefaction

Limin Zhang  
Assistant Professor, Chengdu University of Science and Technology, Chengdu, Sichuan, China

Ting Hu  
Professor, Chengdu University of Science and Technology, Chengdu, Sichuan, China

**ABSTRACT:** The stress-dilatancy relations of sand for the stress paths involved in a complete periodic stress cycle are set up. The plastic potential functions for each loading stage are derived consequently. Based on the idea of using a stress-strain relationship as an alternative strain-hardening law, the drained volume changes under different effective stress paths are derived and verified. A pore pressure generation mechanism which can take into account the dilatancy of soil directly and the related computational model are put forward. The model can calculate the instantaneous and residual pore pressures in sand and depict the liquefaction process of sand quantitatively, especially the dilatancy behaviour.

## INTRODUCTION

There have been a deep understanding of the mechanism of pore pressure generation and development. Wenshao Wang(1980), Martin and Finn(1975), and Dinyi Xie(1986) made great contributions to it respectively. Up to now there is, however, no proper way to calculate the instantaneous pore pressure within a stress cycle, thus it is still difficult to describe the liquefaction process of sand quantitatively. Ishihara(1975), Vaid and Chern(1982) observed the characteristics of liquefaction and made some useful assumptions on these characteristics. Unfortunately, they failed to develop their ideas theoretically. The main reasons are that the pore pressure generation mechanisms cannot take into account the dilatancy of soil and that the assumptions of elastic unloading and elastic reloading in common elastoplastic theories are not applicable to the type of loadings where the cyclic effects dominate, especially when the stress level is high.

In this paper, the authors will deal with these problems of great significance both in theory and practice in cooperation with the liquefaction potential evaluation for the lenses in the ground of Pubugou Power Station. The physical property indexes are listed as following:

specific weight  $G = 2.69$   
in-situ void ratio  $e = 0.65$   
relative density  $D_r = 0.70$   
in-situ water content  $w = 20\%$   
average grain size  $d = 0.15\text{mm}$   
uniformity coefficient  $c = 25.5$   
in-situ dry unit weight  $\gamma = 16.6 \text{ kN/m}^3$

## STRESS-DILATANCY RELATIONS

Rowe(1972) studied the stress-dilatancy relations for compression and extension processes from the energy relations of two particles in contact and expressed them as following

$$\begin{aligned} R &= K_D D & (1) \\ R &= 1/K_D & (2) \end{aligned}$$

in which,  $R$ =stress ratio,  $R=q/\bar{q}$ ,  $D$ =dilatant factor,  $D=d\epsilon/d\epsilon_v$ ,  $q, \bar{q}$ =axial stress and radial stress,  $d\epsilon$ =axial strain increment,  $d\epsilon_v$ =slip volumetric strain increment,  $K_D$ =critical energy ratio. As in other elastoplastic models, Rowe treated the unloading process as elastic rebound. In fact, a great deal of volume compression is observed during unloading process when the effective stress level surpasses the phase transformation line, which shows no common points with an elastic rebound. This is also clearly shown in the effective stress path reversal when the effective stress level reaches the Phase Transformation Line in an undrained test. In order to determine the plastic volume changes during unloading and reloading processes, a series of tests are done, including compression tests with constant  $P$ , cyclic loading test with constant  $P$ , and cyclic shear test with constant  $q$  on a static triaxial apparatus with specimen size  $\phi 3.9 \times 8 \text{ cm}$ , and cyclic extension test with constant  $P$  on a dynamic triaxial apparatus with specimen size  $\phi 5 \times 11 \text{ cm}$ . The stress-dilatancy plots obtained from these tests are shown in Fig. 1. The stress-dilatancy relation of the unloading after compression is represented by CD. After extension, by EA. The unloading stress-dilatancy relations can also be expressed as the following functional relationships respectively,

$$\begin{aligned} R &= K_D (D - D_1) & (3) \\ R &= 1/K_D (D - D_2) & (4) \end{aligned}$$

in which,  $D_1$  and  $D_2$  are material parameters. For the tested sand from the upper lens in the ground of the Pubugou Power Station (Hole No. 35),  $K_D = 3.4$ ,  $D_1 = 2.0$ ,  $D_2 = -2.5$ .

It can be seen from Fig.1 that the stress-dilatancy relations of a complete stress cycle consist of a closed polygon. The stress dilatancy relations of loading and unloading along different effective stress paths with the same loading property are similar with each other. The closed polygon in Fig.1 is unique in statistic aspect.

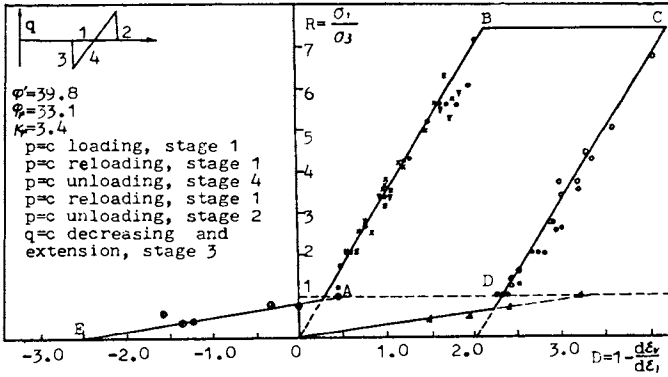


Fig.1 Stress-Dilatancy Relations of the Lens Sand in the Ground of the Pubugou Power Station

Fig. 2 is a plot for a dense sample tested over three cycles at  $q=10$  Lb/sq.in. by Barden and Khayatt (1969). The magnitudes of the strains over the first, second, and third cycles are all very different but despite this fact very similar dilatancy plots result. Similar results have been obtained from multi-cycle tests with  $q$  constant, or with  $q$  constant. Another conclusion can be drawn that the stress-dilatancy relations are not affected by the stress history during cyclic loading process.

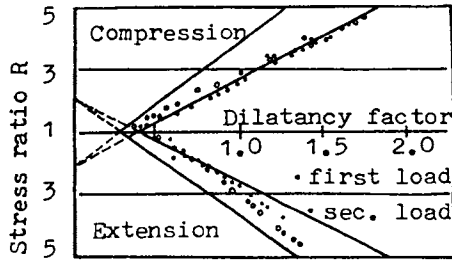


Fig.2 Stress-Dilatancy Plot in Cycling tests (after barden and Khayatt)

#### DRAINED VOLUME CHANGE DETERMINATION

The volumetric strain involved in a stress-dilatancy relation is of the plastic characteristics. The total volumetric strain increment,  $d\varepsilon_v$ , is divided into an elastic component,  $d\varepsilon_v^e$  and a plastic component,  $d\varepsilon_v^p$ .

$$d\varepsilon_v = d\varepsilon_v^e + d\varepsilon_v^p \quad (5)$$

The elastic component  $d\varepsilon_v^e$  can be calculated by means of an elastic rebound bulk modulus,  $K_e$ ,

$$d\varepsilon_v^e = dp / K_e \quad (6)$$

in which,  $dp$  is the effective spherical stress increment. The plastic component can be expressed in terms of the flow rule,

$$d\varepsilon_v^p = d\lambda \frac{g}{p} \quad (7)$$

in which,  $d\lambda$ =theory of strain-hardening law,  $d\lambda = 1/A \cdot f / H \cdot dH$ ;  $H$ =hardening parameter;  $A=f(H)$ ;  $f$ =yield surface  $g$ =plastic potential function. The plastic potential functions corresponding to the four loading stages in Fig. 1 can be derived from the stress-dilatancy relations,

$$g_1 = \sigma_r \sigma_a^{-2K_\mu} \alpha \quad (8)$$

$$g_2 = \sigma_r \sigma_a^{-\frac{\alpha}{2K_\mu}} \quad (9)$$

$$g_3 = \sigma_r \sigma_a^{-\frac{2}{K_\mu} \alpha} \quad (10)$$

$$g_4 = \sigma_r \sigma_a^{-\frac{K_\mu \alpha}{2.5} \frac{\sigma_a}{\sigma_r}} \quad (11)$$

in which,  $\alpha$  is an integration constant. The flow rules for each loading stage are,

$$\frac{d\varepsilon_r}{d\varepsilon_a} = \frac{\partial g}{\partial \sigma_r} / \frac{\partial g}{\partial \sigma_a} \quad (12)$$

$$\frac{d\varepsilon_r}{d\left(\frac{\varepsilon_a}{\sqrt{2K_\mu}}\right)} = \frac{\partial f}{\partial \sigma_r} / \frac{\partial f}{\partial\left(\frac{\sigma_a}{\sqrt{2K_\mu}}\right)} \quad (13)$$

$$\frac{d\varepsilon_r}{d\varepsilon_a} = \frac{\partial f}{\partial \sigma_r} / \frac{\partial f}{\partial \sigma_a} \quad (14)$$

$$\frac{d\varepsilon_r}{d\left(\frac{\varepsilon_a}{\sqrt{\frac{2}{K_\mu}}}\right)} = \frac{\partial f}{\partial \sigma_r} / \frac{\partial f}{\partial\left(\frac{\sigma_a}{\sqrt{\frac{2}{K_\mu}}}\right)} \quad (15)$$

The flow rules can be associative by selecting proper  $\beta$ . There have been many assumptions on the hardening parameter  $H$ . Wenxue Huang(1981) made an excellent summary on these assumptions. Unfortunately, those results are very complicated and lack theoretic basis. The authors here use a nonlinear elastic stress-strain relationship as an alternative of the strain-hardening law,

$$d\varepsilon_r^p = dq / G_s \quad (16)$$

in which,  $d\varepsilon_r^p$  ( $d\varepsilon_r - d\varepsilon_r^e$ ),  $G_s$ =shear modulus. For the first loading stage, the plastic volumetric strain increment can be obtained by the solution of the simultaneous Eq.8, Eq.12, and Eq.16,

$$d\varepsilon_r^p = dq / K_s \quad (17)$$

in which,  $dq$ =shear stress increment;  $K_s$ = shear bulk modulus,

$$K_s = 2G_s(1 + q/2K_\mu \alpha) / (1 - q/K_\mu \alpha) \quad (18)$$

The computed and tested results are shown in Fig.(3-a). In the case of shear test with  $q$  constant, Eq. 16 is not valid, a new stress-strain relationship is developed for it,

$$d\varepsilon_r^p = d\eta / G_\eta$$

in which,  $\eta = q/p$ ,  $G_\eta = G_s + A\eta$ ,  $G_s$  and  $A$  =material parameters. The corresponding volumetric strain increment is,

$$d\varepsilon_v^p = d\eta / K_\eta \quad (19)$$

in which,  $d\eta$  = stress level increment;  $K_r$  = shear bulk modulus,

$$K_r = G_v / (3(1 - 5/(4 + q/(K_r \sigma_r)))) \quad (20)$$

Fig. 3(b) shows the tested and predicted results. It should be noted that the moduli in equations above are determined according to their effective stress paths strictly. The volumetric strain determinations under other effective stress paths are obtained in similar way. It is very flexible to accommodate the different effective stress paths. According to the above equations, plastic volume change develops during unloading and reloading processes, which is an advantage of this elastoplastic theory and has a great significance in predicting the undrained behaviours of soil.

It can also be seen from Fig.3 that soil begins to dilated at the same stress level  $\eta_r$ . The value of  $\eta_r$  can be easily derived from the theory above,

$$\eta_r = 3(K_r - 1) / (2 + K_r) \quad (20)$$

The line with the slope  $\eta_r$  in the  $p$ - $q$  coordinates is called the Phase Transformation Line. The method of determining the line in this paper seems to be easier in comparison with that of Ishihara (1975).  $d\epsilon_v > 0$

when  $\eta < \eta_r$ , while  $d\epsilon_v < 0$  when  $\eta > \eta_r$ .

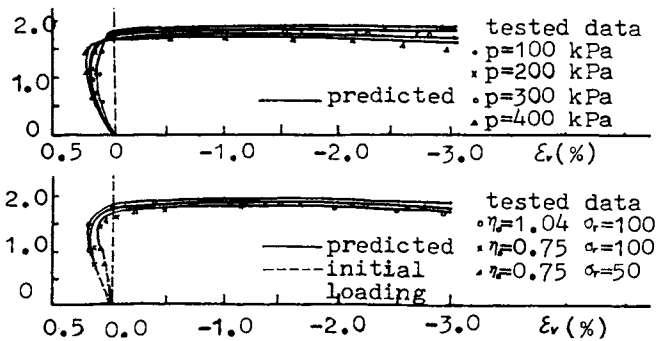


Fig. 3 Volumetric Strain-Stress Level Relationships at (a) Constant  $p$  (b) Constant  $q$

#### MECHANISM OF PORE PRESSURE GENERATION AND DEVELOPMENT

As shown in Fig.4,  $V_1$  and  $V_2$  are two equivoluminal lines. Subjected to external stress increments  $dp$  and  $dq$ , the sand will tend to be denser, with potential volume change  $d\epsilon_v = V_1 - V_2$ . As a result, pore pressure increases in an undrained testing system, which causes the soil skeleton to tend to expand and the testing system to yield. The potential volume change increment,  $d\epsilon_v$ , should be compensated by the corresponding swelling,  $d\epsilon_s$ , and the system compliance,  $d\epsilon_c$ , to abide by the law of volume compatibility of an undrained testing system, i.e.

$$d\epsilon_v - d\epsilon_s - d\epsilon_c = 0 \quad (21)$$

Suppose the potential volume change increment caused by  $dp$  and  $dq$  is equal to the drained volume change increment caused by the same effective stress changes under the same effective stress  $p$  and  $q$ , and the resiliance of the soil skeleton takes place under a constant  $q$ , the pore pressure increment as a response to the stress changes is derived for general stress condition

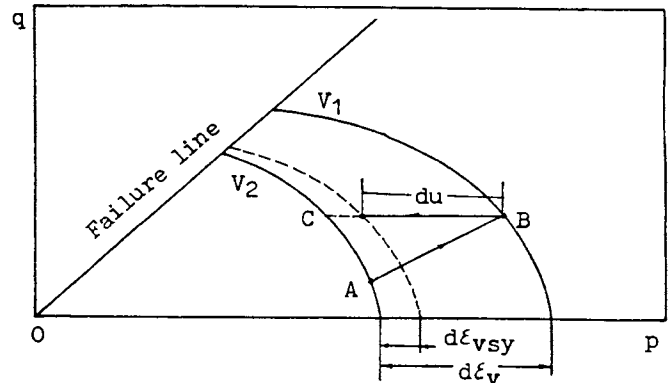


Fig.4 Mechanism of Pore-pressure Generation

$$du = \frac{\frac{dp}{K_r} + C_1 \frac{dq}{K_q}}{\frac{1}{K_r} + \left( \frac{1}{K_r} - \frac{C_2 q}{K_r p^2} \right) (1 + C_3 R')}$$

in which,  $K_r$  = elastic rebound bulk modulus,  $K_q$  = shear bulk modulus corresponding to the specific loading stages,  $C_1$  and  $C_2$  = coefficients for the errors in drained plastic volume changes caused by the testing system, the specimen sizes, and dynamic effects,  $C_3$  = system yield ratio,  $C_2 = (1/k_r - q/k_p) / k_p$ ,  $k_p$  = bulk modulus of system compliance.  $C_3$  is taken as zero for the tested fine sand. The values of the coefficients  $C_1$  and  $C_2$  may be different for each stage of a stress cycle. For the triaxial stress condition with  $q$  constant,  $dp = 1/3 dq$ , the step-by-step calculation using Eq. 22 will result in the instantaneous pore pressure history, therefore, the residual pore pressure development and the numeralized liquefaction process of sand.

#### EXAMPLES OF PORE PRESSURE DEVELOPMENT UNDER CYCLIC LOADING

Fig.(5-a) shows the tested effective stress path of a specimen of the sand lens isotropically consolidated at the confining pressure 100kPa. The amplitude of the uniform symmetric cyclic loading is 44.3 KPa. The stress path in Fig.(5-b) is the predicted effective stress path with Eq.22. The effective stress paths shown in Fig.(5-c) and Fig.(5-d) are the tested and predicted curves of an specimen anisotropically consolidated at the confining pressure 100kPa and the consolidation ratio 1.5. The uniform unsymmetric cyclic loading applied has a maximum compression 112 KPa and a maximum extension 59 KPa. The results of the residual pore pressures in above two cases are shown in Fig.(5-e). As can be seen in Fig.(5-b) and Fig.(5-d) the loading pore pressure increases before the effective stress reaches the Phase Transformation Line, while it decreases after the effective stress surpasses the Phase Transformation Line. The effective stress paths change their directions from anti-clockwise to clockwise. The theoretical predictions have revealed these characteristics. The theoretical predictions have revealed these characteristics. Good agreements have also been obtained between the predicted and the tested residual pore pressures both for the isotropically consolidated specimen and the anisotropically consolidated specimen, as shown in Fig.(5-e). The Phase Transformation Lines are consolidation ratio independent.

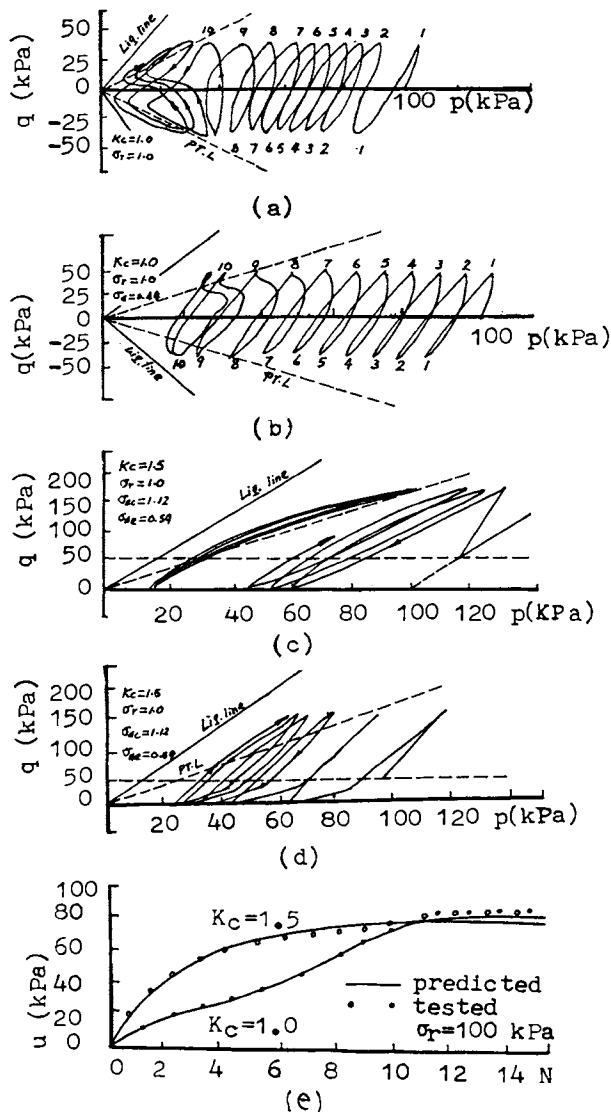


Fig. 5 Tested and Predicted Results of the Pubugou Lens Sand (a) Tested Effective Stress Path( ESP) ,  $\sigma_r=100\text{KPa}$ ,  $K_c=1.0$ ; (b) Predicted ESP,  $\sigma_r=100\text{KPa}$ ,  $K_c=1.0$ ; (c) Tested ESP,  $\sigma_r=1.0$ ,  $K_c=1.5$ ; (d) Predicted ESP,  $\sigma_r=100\text{KPa}$ ,  $K_c=1.5$ ; (e) Tested and Predicted Residual Pore-water Pressures

## CONCLUSIONS

Drained tests with a sand from the upper lens in the ground of the Pubugou Power Station under different stress paths and undrained tests with under cyclic loadings are done. The following conclusions are drawn

1. The stress-dilatancy relations of sand can be generalized from the relations for compression and extension by Rowe et al to a complete stress cycle. The stress-dilatancy relations corresponding to the four stages of a stress cycle consist of a closed polygon which is unique for different stress paths of the same loading stage and for multicyle tests.
2. The elastoplastic theory using alternative flow rules and alternative strain-hardening laws is capable of determining the drained volume changes under different effective stress paths, including the plastic

volume changes during loading and unloading, with special capacity to characterize the dilatancy of sand.

3. The presented pore-water pressure generation mechanism takes the dilatancy of soil into account directly. It leads to a computational model which can evaluate the instantaneous pore-water pressure development of soil with or without initial shear stress, thus, the residual pore-water pressure development and the characteristics of liquefaction processs, esp. the behaviours prior to and after the Phase Transformation Line. The quantitative description of liquefaction process is, no doubt, a progress of the preliminary qualitative studies.

## REFERENCES

- [1] Barden, L. and Khayatt, A.J. "Incremental strain rate ratios and strength of sand in the triaxial test," *Geotechnique*, Vol.16, No.4, 1966.
- [2] Dinyi Xie, "Development mechanism and computation model of transient pore-water pressure in saturated sand," Proc. of the China National Academic Conference on Seismic Resistance of Earth Structure and Soil Foundation, Xian, 1986.
- [3] Ishihara, K. et al. "Undrained deformation and liquefaction of sand under cyclic stresses," *Soils and Foundations*, Vol.15, No.1, 1975.
- [4] Martin, G. R., Finn, W.D.L., and Seed, H. B. . "Fundamentals of liquefaction under cyclic loadings," *JGTD, ASCE*, Vol.101, GT5, 1975.
- [5] Rowe, P.W., "Theoretical meaning and observed values of deformation parameters," *Stress-Strain Behaviour of Soils* (Ed. Parry, R.H.G.), Roscoe Memorial Symposium, Cambridge University, 1972.
- [6] Vaid, Y.P. and Chern, J.C., "Mechanism of deformation during cyclic undrained loading of saturated sands," Proc. of the Conf. on Soil Dynamics and Earthquake Engineering, Southampton, Vol.1, 1982.
- [7] Wenshao Wang, "Some findings in sand liquefaction studies," *Chinese Journal of Geotechnical Engineering*, Vol.2, No.3, 1980.
- [8] Wenxue Huang, *The Engineering Properties of Soils*, Press of Water Conservancy and Hydroelectric Power, Beijing, 1983.P